

# Fragmentation Functions for $K_S^0$ and $\Lambda$ with Complete Quark Flavour Separation

S. Albino

*Institut für Theoretische Physik und Astrophysik,  
Universität Würzburg, 97074 Würzburg, Germany*

B. A. Kniehl and G. Kramer

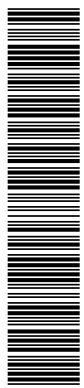
*II. Institut für Theoretische Physik, Universität Hamburg,  
Luruper Chaussee 149, 22761 Hamburg, Germany*

(Dated: October 13, 2005)

## Abstract

We present new sets of next-to-leading order fragmentation functions for the production of  $K_S^0$  and  $\Lambda$  particles from the gluon and from each of the quarks, obtained by fitting to all relevant data sets from  $e^+e^-$  annihilation. The individual light quark flavour fragmentation functions are constrained phenomenologically for the first time by including in the data the light quark tagging probabilities measured by the OPAL Collaboration.

arXiv:hep-ph/0510173 v1 13 Oct 2005



## I. INTRODUCTION

At present, experimental results on inclusive hadron production from  $e^+e^-$  collisions are the most reliable source for the extraction of universal fragmentation functions (FFs)  $D_a^h(x, Q^2)$  (where  $a$  labels the fragmenting parton,  $h$  labels the produced hadron,  $x$  is the fraction of the parton's momentum taken by the produced hadron and  $Q$  is the factorization scale), which are crucial for making predictions for such processes in future experiments, as well as for understanding the non-perturbative mechanism of hadron formation in parton jets. However, the extraction of quark flavour separated FFs from experimental data has not been completely possible due to the lack of data for processes in which the individual light quark flavours are tagged. Therefore, theoretical assumptions between light quark flavour FFs had to be made. Recently, we published sets of FFs [1] for each of the three light charged hadrons, whose quark flavours were completely phenomenologically separated by including the light quark flavour separated measurements from the OPAL collaboration [2] in the data used for the fitting. This more reliable separation in the light quark flavour sector of the FFs via real experimental data is important for the description of hadron production in proton-(anti)proton collisions, for example at the RHIC, Tevatron, LHC and other experiments, because the proton is composed predominantly of light partons.

In this paper, we extend our analysis of Ref. [1] to determine FFs for  $K_S^0$  and  $\Lambda$  production, in which the quark flavours are phenomenologically separated by including, among the available data, the tagging probability measurements for each of the quark flavours for these two particles provided by OPAL in Ref. [2]. FFs for  $K_S^0$  production have been previously obtained in Ref. [3], however since no data was available to separate the light quark flavours, it was assumed that the  $d$  and  $s$  quark FFs were equal. Much data for  $K_S^0$  production can also be well described by using FFs for  $K^\pm$  [1, 4], so it is interesting to verify if these two sets of FFs are really consistent. In Ref. [5], FFs for  $\Lambda$  production were obtained by constraining all light quark flavours to be equal and imposing certain relations between them and the heavy quark FFs, since no data was available at the time to fully constrain the individual quark flavour FFs. A further determination of FFs for  $\Lambda$  production was obtained more recently in Ref. [6], along with FFs for the other octet baryons, again with relations imposed between flavours, but also with some assumptions suggested by fermionic and bosonic statistics. A more reliable determination of these FFs is important due to the

recent data on  $K_S^0$  and  $\Lambda$  production, taken by the STAR Collaboration [7] at BNL RHIC. In particular, next-to-leading order (NLO) calculations deviate considerably from the data for  $\Lambda$  production. For the first time, we present FFs for these particles without imposing constraints on the non-perturbative components (except for the choice of parameterization for the FFs).

## II. METHOD

In all cross section calculations in this paper, used to fit FF parameters to data and to produce comparisons to this data and other data, we use precisely the same method and choice of parameterization, scales etc. as in Ref. [1], and therefore we refer the reader to this paper for details. This includes taking the fitted NLO value  $\Lambda_{\overline{\text{MS}}}^{(5)} = 221$  MeV of Ref. [1]. For each parton, our FFs for  $K_S^0$  production are defined to be those for the production of a single  $K_S^0$  particle, which is equal to the average of those for  $K^0$  and  $\overline{K}^0$ , and our FFs for  $\Lambda$  production are defined to be the sum of those for  $\Lambda^0$  and  $\overline{\Lambda}^0$ . Our FFs incorporate both the intrinsic (non-perturbative) and extrinsic (perturbative, dynamically generated) components of hadron production. It is important to note that our FFs contain intrinsic transitions involving intermediate hadrons occurring over durations much greater than that of the interaction, for example the process  $q + \overline{q} \rightarrow \Sigma^0 + X \rightarrow \Lambda + \gamma + X$  in  $\Lambda$  production noted in Ref. [5], since such processes are not subtracted from the data. Treatment of such effects are beyond the scope of this work.

To obtain FFs for  $K_S^0$  production, we fit to all available  $e^+ + e^- \rightarrow K_S^0 + X$  data, covering a range of centre-of-mass energies  $\sqrt{s}$ , being the untagged data from TASSO at  $\sqrt{s} = 14, 22$  and  $34$  GeV [8] and at  $14.8, 21.5, 34.5, 35$  and  $42.6$  GeV [9], from HRS [10], MARK II [11] and TPC [12] at  $29$  GeV, from TASSO at  $33.3$  GeV [13], from CELLO at  $35$  GeV [14], from TOPAZ at  $58$  GeV [15] and from ALEPH [16], DELPHI [17], OPAL [18] and SLD [19] at  $91.2$  GeV. The data from DELPHI at  $183$  and  $189$  GeV [20] are not included in the fit as will be explained below. In addition, light,  $c$  and  $b$  quark tagged data from SLD at  $91.2$  GeV [19] and  $u, d, s, c$  and  $b$  quark tagged probability measurements from OPAL at  $91.2$  GeV [2] are used to separate the individual quark flavours of the FFs. Likewise, FFs for  $\Lambda$  production are obtained by fitting to all available  $e^+ + e^- \rightarrow \Lambda^0(\overline{\Lambda}^0) + X$  untagged data from TASSO at  $14, 22$  and  $34$  GeV [8], from HRS [21] and MARK II [22] at  $29$  GeV, from

TASSO at 33.3 GeV [13] and at 34.8 and 42.1 GeV [23], from CELLO at 35 GeV [14], from ALEPH [16], DELPHI [24], OPAL [25] and SLD [19] at 91.2 GeV and from DELPHI at 183 and 189 GeV [20]. The individual quark flavours of the FFs are separated using light,  $c$  and  $b$  quark tagged data from SLD at 91.2 GeV [19] and  $u$ ,  $d$ ,  $s$ ,  $c$  and  $b$  quark tagged probability measurements from OPAL at 91.2 GeV [19]. Soft gluon effects [26] cause the DGLAP evolution to fail at small  $x = 2p/\sqrt{s}$ , where  $p$  is the momentum of the observed hadron produced in the final state. Consequently we restrict our analysis to data for which  $x > 0.1$ , which implies that our FFs will not be valid below this  $x$  value. Thus we have a total of 193 data points for  $K_S^0$  production and of 129 for  $\Lambda$  production. The individual systematic errors on the data sets are not given in the literature by these experimental collaborations, which means that, like all previous FF determinations, we are limited to fixing the off-diagonal elements of the covariance matrices for the data sets to zero. We stress however that the experimental constraints on FFs (and  $\alpha_s(M_Z)$ ) would be greatly improved by the inclusion of these correlation effects.

### III. RESULTS

In this section we perform fits to  $K_S^0$  and  $\Lambda$  production data to determine FFs for these particles. In a first analysis, the FF parameters  $N$ ,  $\alpha$  and  $\beta$  for the gluon and each of the 5 quark flavours are released. While an overall good fit is obtained, the fitted initial gluon FFs are negative for both particles. Such a result may be unphysical. Redoing the fits with the initial gluon FFs fixed to zero (so that the evolved gluon FF in each case is generated dynamically from the quarks) gives similar results, implying that the initial gluon FFs are consistent with zero with respect to these data. This is to be expected since the gluon FF only enters the cross section at NLO, and can therefore only be reasonably constrained by more accurate data such as that in Ref. [1]. To obtain a set of FFs in which the gluon FF is reliable, we redo both fits with the initial gluon FF for each particle fixed to some function whose choice and motivation will now be explained. Using the approximation

$$D_a^{K_S^0} = \frac{1}{2} D_b^{K^\pm}, \quad (1)$$

where  $b = u, d$  if  $a = d, u$ , otherwise  $b = a$ , we fix the initial gluon FF for  $K_S^0$  production to half the AKK [1] initial gluon FF for  $K^+ + K^-$  production. For  $\Lambda$  production, it is reasonable

to assume that the gluon FF is related to that of the proton. However, since the valence structure of  $\Lambda$  is  $uds$  compared to  $uud$  for the proton, we assume that this relation holds with an overall suppression factor, which we determine approximately by requiring a good description of the  $pp$  initiated cross section measurements from the STAR collaboration [7] to be discussed later. We find that a good description of such data is achieved if the initial gluon FF for  $\Lambda$  production is fixed in the fit to the AKK initial gluon FF for  $p+\bar{p}$  production suppressed by a factor of 3. Thus the STAR data is in some sense crudely included in the fit, at least in the sense of providing some constraint on the gluon FF for  $\Lambda$  production.

We obtain  $\chi_{\text{DF}}^2 = 1.14$  and  $\chi_{\text{DF}}^2 = 1.39$  for the fits to the  $K_S^0$  and  $\Lambda$  production data, respectively, indicating that both fits are good overall. The quality of the fit to each individual data set is determined by its  $\chi_{\text{DF}}^2$  value, and these are listed in Tables I – IV. The values in Tables I and II show that the agreement with the OPAL tagging probabilities is good. The good agreement with heavy quark tagged data is surprising when compared with our findings of Ref. [1]. For that analysis of light charged hadron production data, although we found good agreement with the DELPHI, SLD and TPC heavy quark tagged data, a poor description of the OPAL heavy quark tagged data was obtained, which, as we suggested, may be due to large angle gluon emission effects. Whatever effect caused this disagreement is clearly not as significant for the  $K_S^0$  and  $\Lambda$  production data we are considering here, although we note that we find a rather large  $\chi_{\text{DF}}^2$  value for  $b$  quark tagged  $K_S^0$  production. The  $\chi_{\text{DF}}^2$  values for  $K_S^0$  production in Table III indicate that each data set is well fitted except the DELPHI data at 183 and 189 GeV which are excluded from the fit. When these data are included, their  $\chi_{\text{DF}}^2$  values remain high (and not much less than those shown in Table III). Such data require further consideration. In any case, only 3 data points of these DELPHI data lie in the region  $x > 0.1$ , so they do not significantly change the size of the data sample used in our fit. We will therefore exclude them in our fit. Table IV shows that unsatisfactory agreement was obtained only with untagged data from DELPHI and  $b$  quark tagged data from SLD, both at  $\sqrt{s} = 91.2$  GeV. The data points from DELPHI at 183 GeV (1 point) and 189 GeV (1 point) for  $\Lambda$  production were excluded for the same reasons as in the case of  $K_S^0$  production, although the point at 183 GeV could be well fitted.

The results for the FF parameters are shown in Table V. The value for  $\alpha$  and/or  $\beta$  may become large because the shape of the FF at small and/or large  $x$  respectively is not well constrained. However, the value of  $N$  is then large to compensate for this. For  $\Lambda$  production,

the initial FF for the  $d$  quark is negative, probably because this initial FF is consistent with zero with respect to the data which constrains it. The initial  $u$  quark FF has a large negative  $\alpha$ , due to a lack of data to constrain this FF at small  $x$ .

The graphical comparison with the quark tagging probabilities is shown in Fig. 1. The curves obtained from our FF set in this analysis (labelled “AKK”) agree well with the data. For  $K_S^0$  production, we also show the curves obtained from the FF set for  $K^\pm$  production in Ref. [1], assuming the relation in Eq. (1). These curves are consistent with these measurements. Also shown are the curves obtained from the FF set for  $K_S^0$  production of Ref. [27] (labelled “GR”). These curves are consistent with the data, showing the validity of these authors’ method of obtaining these FFs from the Monte Carlo generator HERWIG. We note that curves calculated from the FFs for  $K^\pm$  production from Ref. [27] (also obtained from HERWIG) using the same assumptions (Eq. (1)) are also consistent with the  $K_S^0$  quark tagging probabilities. For  $\Lambda$  production, we also show the curves obtained from the FF set presented in Ref. [5] (labelled “FSV”). These are generally consistent with the data except for the  $s$  and  $c$  quark tagged data. Unfortunately, we are unable to show the predictions from the FF set for  $\Lambda$  production of Ref. [6], since the Mellin transform of the parameterization used therein, that is required for our Mellin inversion calculation of the cross section [1], cannot be obtained in closed form. Such predictions require a NLO  $x$  space program. The comparison with the differential cross sections is shown in Figs. 2 and 3. For  $K_S^0$  production, the disagreement of the calculation with the DELPHI data point at 183 GeV can be seen, and, of the two points at 189 GeV, with the one that is the higher in  $x$ . For  $\Lambda$  production, the failure of the description of the data point at 189 GeV can be seen. Note that the DELPHI data for  $\Lambda$  production at 91.2 GeV that gave a high  $\chi_{\text{DF}}^2$  has rather small errors. Finally, in Fig. 3 the cross section for  $\Lambda$  production in the region  $x < 0.1$  is not shown since large negative values were obtained there. This results from the large negative value for  $\alpha$  in the FF for the  $u$  quark discussed earlier.

The quark tagged data from SLD is shown in Figs. 4 and 5, together with the calculation of these cross sections from the FF sets of this analysis. Reasonable agreement is found with most of the data. However, in Fig. 5 there is significant disagreement with the interval from the  $b$  quark tagged cross section for  $\Lambda$  production whose central point is just below  $x = 0.4$ . The light flavour quark tagged cross section in this figure is large and negative in the region  $x < 0.1$ , again due to the large negative value for  $\alpha$  in the FF for the  $u$  quark.

We find that the large initial strange and charm quark FFs for  $\Lambda$  production render the other quark FFs negligible at large  $x$ , and this is reflected at higher scale in the OPAL tagging probabilities at large  $x_p$ . This finding was not observed in Ref. [5], where the light quark FFs were constrained to be equal. This should make a significant difference to hadron production data from proton-(anti)proton collisions, where the light quark PDFs are important.

To test our FFs, we use them to predict the recent preliminary measurements for  $pp$  initiated cross sections at  $\sqrt{s} = 200$  GeV from the STAR Collaboration [7] and for  $p\bar{p}$  initiated cross sections at  $\sqrt{s} = 630$  GeV for  $K_S^0$  and  $\Lambda$  production from the UA1 Collaboration [28] at the CERN SPS. We use the NLO coefficient functions for this process from Ref. [29], and the CTEQ6M parton distribution functions from Ref. [30]. Figure 6 shows the results for  $K_S^0$  production, which are very similar to those obtained in a similar plot in Ref. [1], as is to be expected from the similarity between the two AKK curves of Fig. 1. While good agreement with STAR data is found, some other effects are required for the description of the UA1 data. Figure 7 shows the results for  $\Lambda$  production. As discussed earlier, the STAR data were used to motivate the choice of the initial gluon FF: Firstly, fixing the initial gluon FF to that of the AKK proton from Ref. [1] and performing a fit to the  $e^+e^-$  data, we found that the description of the STAR data was too high by a factor of about 3. Since we also found that these data are dominated by the gluon FF at low factorization scale, we divided this choice of the initial gluon FF by this factor and redid the fit (i.e. fitted the initial quark FFs) to get our final FF set for  $\Lambda$  production. The plot shows good agreement with both STAR and UA1 data within the theoretical errors.

#### IV. CONCLUSIONS

We have obtained FFs for  $K_S^0$  and  $\Lambda$  production by fitting to data from  $e^+e^-$  collisions over a wide range of  $\sqrt{s}$  values, from 14 to 91.2 GeV. To separate the light quark flavour FFs, and to improve the determination of the heavy ones, we have included for the first time the quark tagging probabilities from Ref. [2]. For  $K_S^0$  production, we find good agreement with the FFs from Ref. [27] and the FFs for  $K^+ + K^-$  production from Ref. [1] (using Eq. (1) in the latter case) adding support to the reliability of the data of Ref. [2]. For  $\Lambda$  production, we found that the light quark flavour FFs are significantly different at large  $x$ , with the initial strange quark FF dominating over the remaining quark FFs.

In both cases the initial gluon FF is fixed in the fit. For  $K_S^0$  production, we use the AKK initial gluon FF for  $K^\pm$  (divided by 2). This leads to a good description of the  $pp$  initiated STAR data for  $K_S^0$  production, but a bad description of the UA1 data. This problem was also found in Ref. [1] using the AKK FFs for  $K^\pm$  production via Eq. (1). For  $\Lambda$  production, we use the AKK initial gluon FF for  $p/\bar{p}$  production, after dividing by a factor of 3. This factor is chosen to give a good description of the STAR data for  $\Lambda$  production, and also leads to a good description of the UA1 data. Since such data constrains the gluon well at low  $p_T$ , it should in future analyses be directly included in the list of data fitted to. However, currently the calculation, which implements Monte Carlo integration, is too slow to obtain fitted FFs in a reasonable time.

In order to make predictions, our fitted FF's over the range  $0.1 < x < 1$  and  $M_0 < M_f < 200$  GeV can be obtained from the FORTRAN routines at <http://www.desy.de/~simon/AKK2005FF.html>, which are calculated using cubic spline interpolation from a linear grid in  $x$  and linear interpolation from a linear grid in  $\ln\sqrt{s}$ .

### Acknowledgments

The authors would like to thank M. Heinz for providing them with the preliminary numerical values for the measurements of  $K_S^0$  and  $\Lambda$  production in  $pp$  collisions from the STAR collaboration shown graphically in Ref. [7]. This work was supported in part by the Deutsche Forschungsgemeinschaft through Grant No. KN 365/5-1 and by the Bundesministerium für Bildung und Forschung through Grant No. 05 HT4GUA/4.

- 
- [1] S. Albino, B. A. Kniehl, G. Kramer, Nucl. Phys. B 725 (2005) 181.
  - [2] G. Abbiendi *et al.* [OPAL Collaboration], Eur. Phys. J. C 16 (2000) 407.
  - [3] J. Binnewies, B. A. Kniehl, G. Kramer, Phys. Rev. D 53 (1996) 3573.
  - [4] B. A. Kniehl, G. Kramer, B. Pötter, Nucl. Phys. B 582 (2000) 514.
  - [5] D. de Florian, M. Stratmann, W. Vogelsang, Phys. Rev. D 57 (1998) 5811.
  - [6] C. Bourrely and J. Soffer, Phys. Rev. D 68 (2003) 014003.
  - [7] M. Heinz [STAR Collaboration], J. Phys. G 31 (2005) S1011 (preliminary data).
  - [8] M. Althoff *et al.* [TASSO Collaboration], Z. Phys. C 27 (1985) 27.



- [9] W. Braunschweig *et al.* [TASSO Collaboration], *Z. Phys. C* 47 (1990) 167.
- [10] M. Derrick *et al.* [HRS Collaboration], *Phys. Rev. D* 35 (1987) 2639.
- [11] H. Schellman *et al.* [MARK II Collaboration], *Phys. Rev. D* 31 (1985) 3013.
- [12] H. Aihara *et al.* [TPC/Two Gamma Collaboration], *Phys. Rev. Lett.* 53 (1984) 2378.
- [13] R. Brandelik *et al.* [TASSO Collaboration], *Phys. Lett. B* 105 (1981) 75.
- [14] H. J. Behrend *et al.* [CELLO Collaboration], *Z. Phys. C* 46 (1990) 397.
- [15] R. Itoh *et al.* [TOPAZ Collaboration], *Phys. Lett. B* 345 (1995) 335.
- [16] R. Barate *et al.* [ALEPH Collaboration], *Phys. Rept.* 294 (1998) 1.
- [17] P. Abreu *et al.* [DELPHI Collaboration], *Z. Phys. C* 65 (1995) 587.
- [18] G. Abbiendi *et al.* [OPAL Collaboration], *Eur. Phys. J. C* 17 (2000) 373.
- [19] K. Abe *et al.* [SLD Collaboration], *Phys. Rev. D* 59 (1999) 052001.
- [20] P. Abreu *et al.* [DELPHI Collaboration], *Eur. Phys. J. C* 18 (2000) 203 [Erratum-*ibid.* C 25 (2002) 493].
- [21] P. Baringer *et al.* [HRS Collaboration], *Phys. Rev. Lett.* 56 (1986) 1346.
- [22] C. de la Vaissiere *et al.* [MARK II Collaboration], *Phys. Rev. Lett.* 54 (1985) 2071 [Erratum-*ibid.* 55 (1985) 263].
- [23] W. Braunschweig *et al.* [TASSO Collaboration], *Z. Phys. C* 45 (1989) 209.
- [24] P. Abreu *et al.* [DELPHI Collaboration], *Phys. Lett. B* 318 (1993) 249.
- [25] G. Alexander *et al.* [OPAL Collaboration], *Z. Phys. C* 73 (1997) 569.
- [26] Y. L. Dokshitzer, V. A. Khoze, A. H. Mueller, S. I. Troian, *Basics of perturbative QCD* (Editions Frontières, Gif-sur-Yvette, 1991)
- [27] M. Greco and S. Rolli, *Phys. Rev. D* 52 (1995) 3853.
- [28] G. Bocquet *et al.* [UA1 Collaboration], *Phys. Lett. B* 366 (1996) 441.
- [29] F. Aversa, P. Chiappetta, M. Greco, J.Ph. Guillet, *Phys. Lett. B* 210 (1988) 225;  
F. Aversa, P. Chiappetta, M. Greco, J.Ph. Guillet, *Phys. Lett. B* 211 (1988) 465;  
F. Aversa, P. Chiappetta, M. Greco, J.Ph. Guillet, *Nucl. Phys. B* 327 (1989) 105.
- [30] D. Stump, J. Huston, J. Pumplin, W.-K. Tung, H.-L. Lai, S. Kuhlmann, J.F. Owens [CTEQ Collaboration], *JHEP* 10 (2003) 046.

TABLE I:  $\chi_{\text{DF}}^2$  values obtained from the measured quark tagging probabilities for  $K_S^0$  production,  $\eta_a^K$ , at  $\sqrt{s} = 91.2$  GeV in Ref. [2].

$a$	$d$	$u$	$s$	$c$	$b$
$\chi_{\text{DF}}^2$	0.27	1.38	0.54	1.77	2.36

TABLE II:  $\chi_{\text{DF}}^2$  values obtained from the measured quark tagging probabilities for  $\Lambda$  production,  $\eta_a^\Lambda$ , at  $\sqrt{s} = 91.2$  GeV in Ref. [2].

$a$	$d$	$u$	$s$	$c$	$b$
$\chi_{\text{DF}}^2$	1.05	1.00	0.29	1.39	1.02

TABLE III: CM energies, types of data and  $\chi_{\text{DF}}^2$  values for various samples of  $K_0^S$  production measurements. Samples not used in the fits are marked by asterisks. The columns are labelled by the quarks that were tagged in the measurements ( $q$  implies no tagging).

$\sqrt{s}$ [GeV]	tagged: $q$	uds	$c$	$b$
14.0	1.82 [8]			
14.8	2.65 [9]			
21.5	0.69 [9]			
22.0	0.99 [8]			
29.0	1.27 [10] 0.40 [11] 0.16 [12]			
33.0	0.82 [13]			
34.0	1.33 [8]			
34.5	1.89 [9]			
35.0	0.30 [9] 1.64 [14]			
42.6	1.02 [9]			
58.0	0.01 [15]			
91.2	0.33 [16] 0.57 [17] 0.31 [18] 1.13 [19]	0.93 [19]	0.54 [19]	1.85 [19]
183.0	21.87 [20]*			
189.0	4.41 [20]*			

TABLE IV: CM energies, types of data and  $\chi_{\text{DF}}^2$  values for various samples of  $\Lambda$  production measurements. Samples not used in the fits are marked by asterisks. The columns are labelled by the quarks that were tagged in the measurements ( $q$  implies no tagging).

$\sqrt{s}$ [GeV] \backslash tagged:	$q$	uds	$c$	$b$
14.0	0.73 [8]			
22.0	0.73 [8]			
29.0	1.19 [21] 0.83 [22]			
33.0	1.59 [13]			
34.0	1.85 [8]			
34.8	2.29 [23]			
35.0	0.88 [14]			
42.1	0.90 [23]			
91.2	0.43 [16] 4.05 [24] 0.47 [25] 0.33 [19]	1.63 [19]	1.54 [19]	3.70 [19]
183.0	4.89 [20]*			
189.0	16.34 [20]*			

TABLE V: Values and errors of  $N$ ,  $\alpha$  and  $\beta$  resulting from the fit.

Hadron	Flavour	$N$	$\alpha$	$\beta$
$K_S^0$	$d$	0.0297	-0.949	0.0953
	$u$	1.29	0.137	4.53
	$s$	0.560	-0.283	1.43
	$c$	8.43	0.550	6.04
	$b$	28.8	0.574	13.5
	$g$ (fixed)	7.96	2.72	2.45
$\Lambda$	$d$	-16.7	-0.169	20.2
	$u$	0.0016	-3.67	4.27
	$s$	46043	9.27	9.11
	$c$	156	2.71	9.51
	$b$	244	2.15	15.6
	$g$ (fixed)	0.289	0.130	0.854

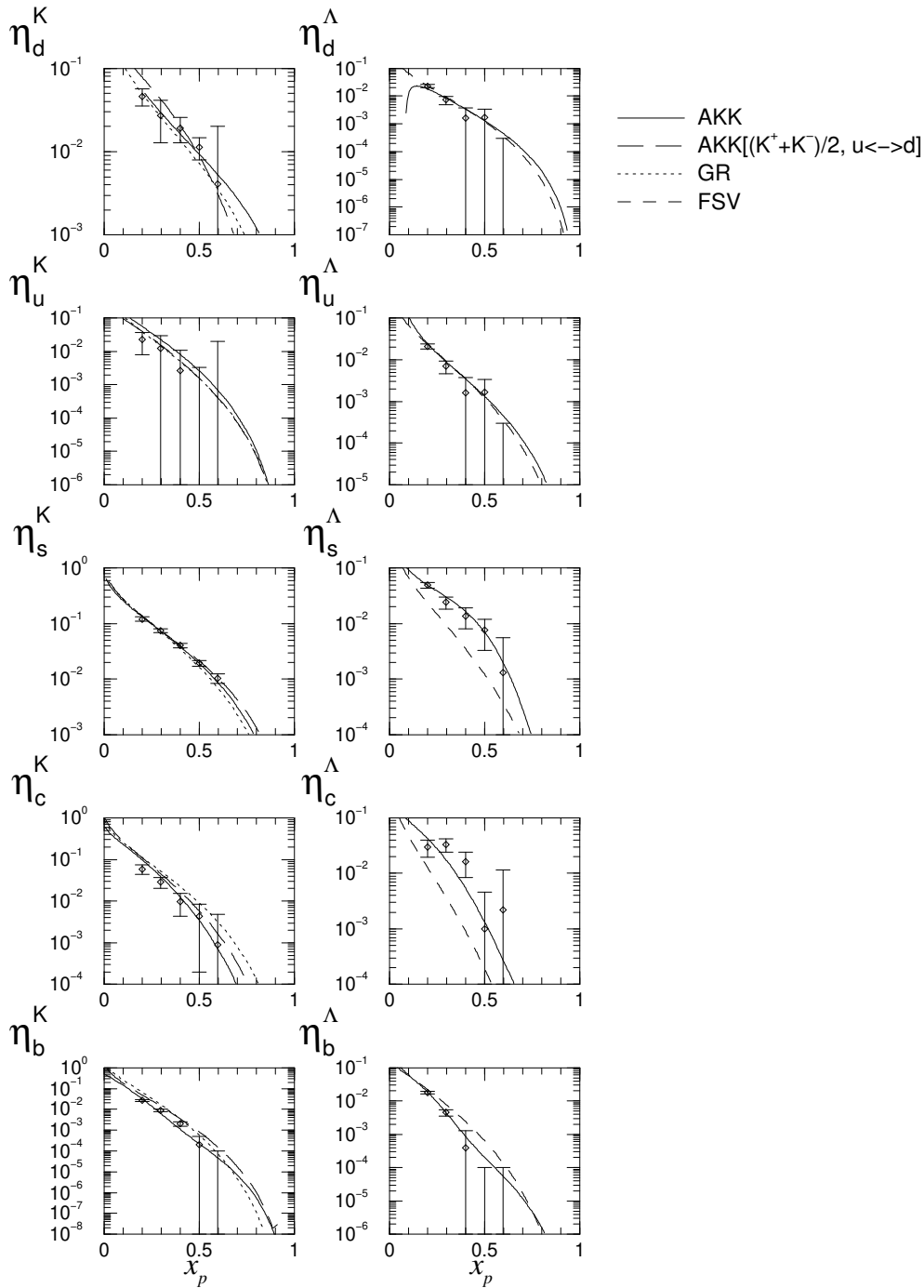


FIG. 1: Quark tagging probabilities  $\eta_a^h(x_p, s)$  at  $\sqrt{s} = 91.2$  GeV. The solid curves labelled “AKK” are calculated from our FF set for  $K_S^0$  production in the graphs on the left hand side and our FF set for  $\Lambda$  production in the graphs on the right hand side. The curves of the same label from the  $K^\pm$  FF set in Ref. [1] (after interchanging  $u$  and  $d$ ) are also shown. In addition, we show the prediction for  $K_S^0$  production from the  $K_S^0$  FF set of Ref. [27] (labelled “GR”) and the prediction for  $\Lambda$  production from the  $\Lambda$  FF set of Ref. [5] (labelled “FSV”). The corresponding measured OPAL probabilities of Ref. [2] are also shown.

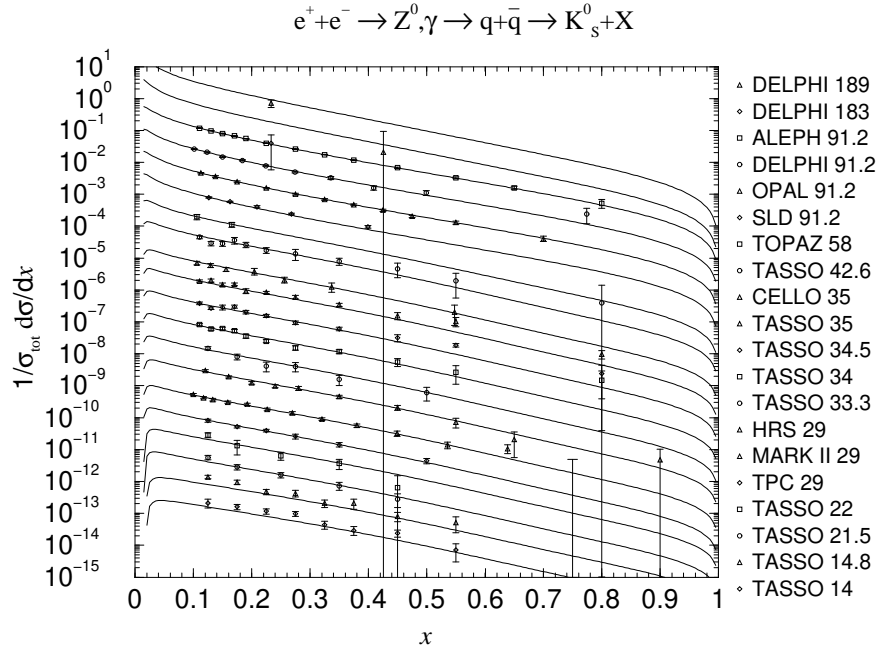


FIG. 2: Normalized differential cross section of inclusive  $K_S^0$  production. The curves are calculated from the FFs obtained in our analysis, at the various energies of the data shown. Each curve and the corresponding data are rescaled relative to the nearest upper one by a factor of  $1/5$ .

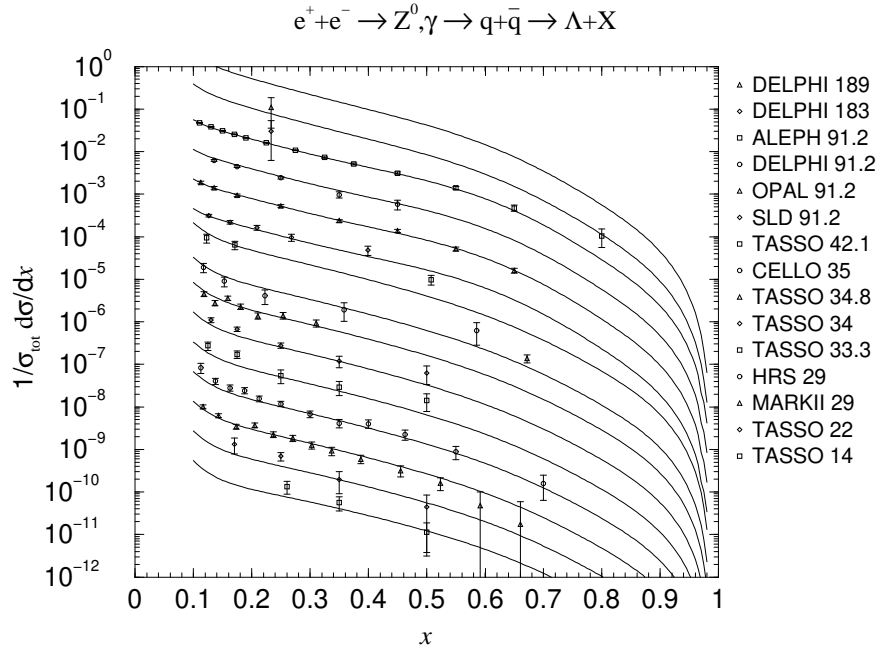


FIG. 3: Normalized differential cross section of inclusive  $\Lambda$  production. The curves are calculated from the FFs obtained in our analysis, at the various energies of the data shown. Each curve and the corresponding data are rescaled relative to the nearest upper one by a factor of  $1/5$ .

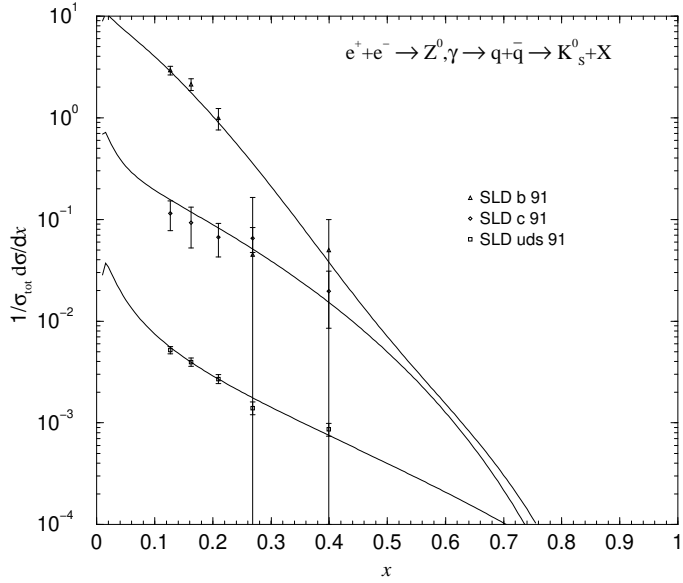


FIG. 4: Normalized quark tagged differential cross sections for inclusive  $K_S^0$  production compared with corresponding data from SLD [19]. The curves are calculated from the FFs obtained in our analysis. Each curve and the corresponding data are rescaled relative to the nearest upper one by a factor of  $1/20$ .

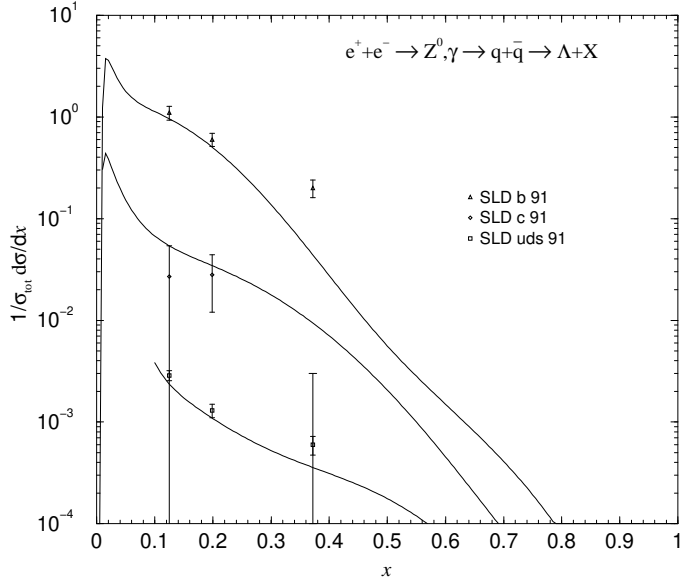


FIG. 5: Normalized tagged differential cross sections for inclusive  $\Lambda$  production compared with corresponding data from SLD [19]. The curves are calculated from the FFs obtained in our analysis. Each curve and the corresponding data are rescaled relative to the nearest upper one by a factor of  $1/20$ .



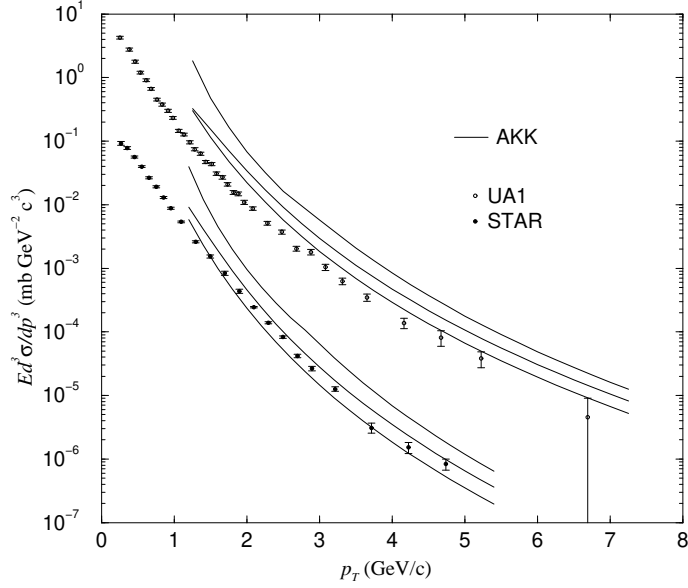


FIG. 6: The invariant differential cross section for inclusive  $K_S^0$  production in  $pp$  and  $p\bar{p}$  collisions. Preliminary data from the STAR Collaboration [7] at  $\sqrt{s} = 200$  GeV (divided by a factor of 30 for clarity) and data from the UA1 Collaboration [28] at  $\sqrt{s} = 630$  GeV are shown, together with their predictions using the FFs obtained in this paper. In the latter case, the upper, central and lower curves are calculated with a renormalization and factorization scale of  $\mu = M_f = p_T/2$ ,  $p_T$  and  $2p_T$  respectively.

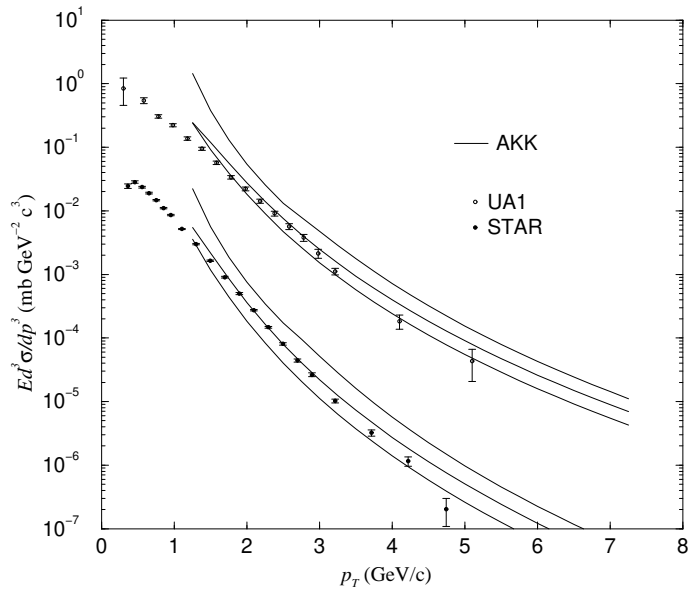


FIG. 7: As in Fig. 6, but for  $\Lambda$  production.